

# Geophysical Research Letters

## RESEARCH LETTER

10.1029/2020GL090167

### Key Points:

- Visibility improvement is not obvious in eastern China despite strict emission control
- Nitrate proportion in PM<sub>2.5</sub> has substantially increased due to unbalanced precursor emission control
- Increased nitrate proportion and humidity enhance aerosol hygroscopicity and extinction efficiency

### Supporting Information:

- Supporting Information S1

### Correspondence to:

X. Huang,  
xinhuang@nju.edu.cn

### Citation:

Liu, J., Ren, C., Huang, X., Nie, W., Wang, J., Sun, P., et al. (2020). Increased aerosol extinction efficiency hinders visibility improvement in eastern China. *Geophysical Research Letters*, 47, e2020GL090167. <https://doi.org/10.1029/2020GL090167>

Received 5 AUG 2020

Accepted 30 SEP 2020

Accepted article online 7 OCT 2020

Jingyi Li and Chuanhua Ren contributed equally to this work.

### Author Contributions:

**Conceptualization:** Xin Huang, Aijun Ding

**Data curation:** Jingyi Liu, Chuanhua Ren, Wei Nie, Jiaping Wang, Peng Sun, Xuguang Chi




**Supervision:** Aijun Ding

**Writing – original draft:** Jingyi Liu, Chuanhua Ren, Xin Huang

**Writing – review & editing:** Jingyi Liu, Chuanhua Ren, Xin Huang

©2020. American Geophysical Union.  
All Rights Reserved.

## Increased Aerosol Extinction Efficiency Hinders Visibility Improvement in Eastern China

Jingyi Liu<sup>1,2</sup>, Chuanhua Ren<sup>1,2</sup>, Xin Huang<sup>1,2</sup> , Wei Nie<sup>1,2</sup> , Jiaping Wang<sup>1,2</sup>, Peng Sun<sup>1,2</sup>, Xuguang Chi<sup>1,2</sup>, and Aijun Ding<sup>1,2</sup> 

<sup>1</sup>School of Atmospheric Sciences, Nanjing University, Nanjing, China, <sup>2</sup>Jiangsu Provincial Collaborative Innovation Center for Climate Change, Nanjing, China

**Abstract** Though China has witnessed substantial particular matter pollution mitigation owing to the strict emission control in recent years, the frequency of haze events with low visibility is not improved as much as expected, especially in cold seasons. Here, 6-year wintertime observations, satellite retrievals, a thermodynamic model, and theoretical calculation were integrated to better understand the complex influence of aerosol chemical composition and hygroscopic behaviors on visibility impairment. We found that the proportion of nitrate in aerosol mass concentration increased by approximately 10% from 2013 to 2018. Such a transition in aerosol chemical compositions together with increasing ambient humidity in past years jointly enhanced aerosol extinction efficiency, and the elevated proportion of nitrate played an increasingly critical role after 2017. The increased aerosol extinction efficiency is responsible for the less improved visibility despite large decrease in aerosol mass concentrations in eastern China.

**Plain Language Summary** Atmospheric aerosol degrades regional visibility as a result of light extinction, which is highly linked with aerosol chemical composition and particle size growth in humid environment. Due to a much sharper drop of sulfur emission than nitrogen emission in China, aerosol has become increasingly nitrate-dominant. The transition in aerosol chemical compositions together with increasing ambient humidity in past years may jointly alter aerosol hygroscopic behaviors and enhance aerosol extinction efficiency. In consequence, although substantial mitigation of aerosol pollution has been achieved in recent years, hazy days with low visibility still frequently occur in eastern China.

## 1. Introduction

Atmospheric aerosol, especially fine particle (PM<sub>2.5</sub>), has drawn increasing attention due to its negative impacts on both air quality and human health (Brook et al., 2010; Kim et al., 2015). As one of the most important pollutants suspended in the atmosphere, aerosol directly scatters or absorbs incident solar radiation and thus deteriorates visibility, which then triggers the well-known “haze” pollution in emission-intensive regions like China (An et al., 2019; Chang et al., 2009; Li et al., 2016). The visibility impairment due to aerosol is closely related to its ambient concentration, chemical composition, as well as hygroscopic growth under high humidity (Kuang et al., 2016; Malm & Kreidenweis, 1997). Among all the chemical components of PM<sub>2.5</sub>, secondary inorganic compositions like sulfate, nitrate, and ammonium (SNA) have been indicated to play a dominant role in light extinction and resultant visibility deterioration because of its high mass loading and hygroscopic behavior (Tombach & McDonald, 2004).

China, one of the fast-developing countries across the world, has witnessed severe air pollution in recent decades. The annual mean concentration of PM<sub>2.5</sub> in 31 provincial capital cities reached up to 75 μg/m<sup>3</sup> in 2013, far more than 10 μg/m<sup>3</sup> which is recommended as the standard level by the World Health Organization (WHO) (Liu et al., 2019). During the winter hazy days, PM<sub>2.5</sub> concentration usually exceeded 500 μg/m<sup>3</sup> in eastern China and SNA generally contributed more than 50% to the total mass concentration (Ding et al., 2016; World Health Organization, 2006), consequently leading to an extremely poor visibility (a few hundred meters) and frequent haze pollution (Zheng et al., 2016). Such a high level of SNA concentration could be attributed to multiple reasons. On the one hand, due to huge energy consumption and agricultural production, emissions of SNA precursors, namely, sulfur dioxide (SO<sub>2</sub>), nitrogen oxides (NO<sub>x</sub>), and ammonia (NH<sub>3</sub>), are quite intensive in China (Zhang et al., 2012, 2015). On the other hand, stagnant meteorological condition and concentrated gas precursors tend to accelerate the heterogeneous reaction and then

chemical production of SNA (Huang et al., 2012; Huang, Ding, Gao, et al., 2020; Huang, Ding, Wang, et al., 2020; Xie et al., 2015).

To mitigate haze pollution, China has implemented the toughest-ever clean air policy across the country since the year of 2013. As expected, concentrations of air pollutants have dropped significantly after the implementation (China State Council, 2013). The annual mean concentration of PM<sub>2.5</sub> for 31 provincial capital cities has declined from 75  $\mu\text{g}/\text{m}^3$  in 2013 to 48  $\mu\text{g}/\text{m}^3$  in 2017. It is also demonstrated by China's emission estimation, from 2013 to 2017, national emissions of SO<sub>2</sub>, NO<sub>x</sub>, and primary PM<sub>2.5</sub> decreased by 59%, 21%, and 33% (Ding et al., 2019; Wang, Lyu, et al., 2019; Zhang, Zheng, et al., 2019), respectively. In Nanjing, a city located in the Yangtze River Delta (YRD) with more strict emission reduction, 5-year reduction of SO<sub>2</sub> concentration reached 70%–80% and showed a significantly higher decrease in comparison with NO<sub>x</sub> (Ding et al., 2019). As a consequence, a larger reduction in sulfate than nitrate was demonstrated by both in situ observations and model simulations (China State Council, 2013; Ding et al., 2019; Zhang, Zheng, et al., 2019).

However, it is worth noting that the atmospheric visibility seems less improved even though pollutant emission has dropped rapidly and PM<sub>2.5</sub> concentration has substantially decreased, particularly in winter (Ding et al., 2019; Huang, Ding, Gao, et al., 2020; Huang, Ding, Wang, et al., 2020; Li, Liao, et al., 2019). For instance, it has been found that PM<sub>2.5</sub> decreased from 52  $\mu\text{g}/\text{m}^3$  in 2013 to 33  $\mu\text{g}/\text{m}^3$  in 2018 in southern China, but the frequency of low visibility events barely changed (~5% decrease) (Xu et al., 2020). The nonlinear response of visibility to PM<sub>2.5</sub> concentration was also observed in the North China Plain, which could be attributed to varying meteorological conditions as well as aerosol chemical composition (Zou et al., 2018). As indicated, SNA, which dominates PM<sub>2.5</sub> mass concentration and attenuation of incident solar radiation, has undergone great transitions from 2013 to 2017 due to disparities in SO<sub>2</sub> and NO<sub>x</sub> reduction (Zheng et al., 2018). Measurements in many places have revealed the fact that secondary aerosol in PM<sub>2.5</sub> has changed from sulfate-dominant to nitrate-dominant (China State Council, 2013; Li, Cheng, et al., 2019; Zhao, Wang, et al., 2019). How the chemical composition transition impact atmospheric visibility and haze pollution in China is still not well understood. Considering that visibility deterioration is currently one of the biggest environmental challenge facing eastern China, this work aims to shed more light on less visibility improvement than expected from the perspective of aerosol chemical composition as well as humidity condition by combining long-term field measurements, theoretical calculations together with a thermodynamic model.

## 2. Data Sets and Methods

### 2.1. In Situ Measurements on PM<sub>2.5</sub> and Its Chemical Composition

Measurements on PM<sub>2.5</sub> concentration are recorded hourly at more than 1,500 stations of China's air quality monitoring networks. All these ground-based observations are archived at an air monitoring data center of Ministry of Ecology and Environment of China, which are collected to derive the spatial distribution and temporal variations of PM<sub>2.5</sub> concentration in this study. In addition to PM<sub>2.5</sub> concentration, its chemical compositions are routinely observed at the Station for Observing Regional Processes of the Earth System (SORPES) in Nanjing, which is a regional background station in the western part of YRD region (32°07'14" N, 118°57'10" E) (Ding et al., 2013, 2019). The station is located on the top of a 40-m hill, inside Nanjing University Xianlin Campus, 20 km northeast of downtown Nanjing (Shen et al., 2018). At this station, meteorological field, PM<sub>2.5</sub> mass concentration, and its precursors are measured continuously since 2011. More species, such as aerosol chemical compositions, including black carbon (BC), organic carbon (OC), sulfate (SO<sub>4</sub><sup>2-</sup>), nitrate (NO<sub>3</sub><sup>-</sup>), ammonium (NH<sub>4</sub><sup>+</sup>), potassium (K<sup>+</sup>), and calcium (Ca<sup>2+</sup>), have been measured since the year of 2013 (Ding et al., 2019; Wang et al., 2018; Xie et al., 2015). PM<sub>2.5</sub> mass concentration is measured by the online analyzer based on the light scattering and beta-ray absorption method (Thermo Fisher Scientific, Model 5030 SHARP, USA). The water-soluble inorganic ions are detected by the Monitor for aerosols and gases in Ambient air (MARGA; Metrohm, Switzerland). BC concentration is observed using a seven-wavelength aethalometer (AE-31, Magee Scientific), and the data at the wavelength of 880 nm were used in this study (Shen et al., 2018). The size distribution and number concentration of aerosol particles were averaged winter values measured with a differential mobility particle sizer (DMPS) (Qi et al., 2015). All the instrumentations at this station are detailed in previous studies (Ding et al., 2013, 2019). Furthermore, atmospheric visibility is obtained from the nearest meteorological station (32°22'N,

118°51'E). Given that the atmospheric visibility during rainy days saturated with water vapor is no longer substantially influenced by PM<sub>2.5</sub>, thus all rainy-day data were not taken into account in this work.

## 2.2. Theoretical Description of Aerosol Hygroscopic Behavior

Hygroscopic deliquescence occurs with most hydrophilic aerosols as the ambient relative humidity (RH) increases. The aerosol particles exist in solid form until the ambient RH reaches a threshold value, which is defined as deliquescence relative humidity (DRH). Once the DRH is reached, the solid particle will spontaneously absorb atmospheric moisture causing a rapid increase in particle size and then gradually transform to saturated aqueous solution. The DRH value of atmospheric aerosol varies with ambient temperature and chemical species (Seinfeld & Pandis, 2016; Tang et al., 2019). For multicomponent aerosols, their deliquescence threshold is called multicomponent deliquescence relative humidity (MDRH). In this work, we calculated the MDRH of hydrophilic aerosol consisting of NH<sub>4</sub>NO<sub>3</sub> and (NH<sub>4</sub>)<sub>2</sub>SO<sub>4</sub>, which are common hygroscopic composition of aerosols in China.

Following the methods of Wexler and Seinfeld (1991), for the NH<sub>4</sub>NO<sub>3</sub>-(NH<sub>4</sub>)<sub>2</sub>SO<sub>4</sub>-H<sub>2</sub>O system, when the two salts are respectively saturated, the water activity of the system are shown below:

For the system saturated with (NH<sub>4</sub>)<sub>2</sub>SO<sub>4</sub> is

$$a_w(m_{\text{NH}_4\text{NO}_3}) = 0.8113 \exp \left\{ -\frac{18}{1000} \left[ 2m_{\text{NH}_4\text{NO}_3} - 0.037m_{\text{NH}_4\text{NO}_3}^2 - 2m_{(\text{NH}_4)_2\text{SO}_4} \ln \left( \frac{1+X}{2-2X} \right) \right] \right\}$$

And for the system saturated with NH<sub>4</sub>NO<sub>3</sub> is

$$a_w(m_{(\text{NH}_4)_2\text{SO}_4}) = 0.7205 \exp \left\{ -\frac{18}{1000} \left[ 3m_{\text{NH}_4\text{NO}_3} + 0.1035m_{(\text{NH}_4)_2\text{SO}_4}^2 - 2m_{\text{NH}_4\text{NO}_3} \ln \left( \frac{2}{X} - 1 \right) \right] \right\}$$

where  $a_w(\text{specie})$  and  $m(\text{specie})$  are the water activity and molality of the two species in the solution respectively,  $X = m_{\text{NH}_4\text{NO}_3} / (m_{\text{NH}_4\text{NO}_3} + m_{(\text{NH}_4)_2\text{SO}_4})$  is the relative mole fraction of dissolved NH<sub>4</sub>NO<sub>3</sub>. The detailed derivation of the above results is given in supporting information, Text S1. The water activity as a function of X is shown in Figure 4a.

As discussed above, hygroscopicity of multicomponent aerosol particles varies with the chemical composition of the aerosol, which will lead to different particle growth size under the same RH.

Particle growth factor (GF) is the ratio of the particle diameter after hygroscopic growth at a given RH to its dry diameter for quantifying aerosol particle hygroscopicity, which can be expressed as  $D_p/D_0$ . The aerosol particle diameter at a specific RH can be calculated by the Köhler equation, which describes the relationship between the equilibrium size of solution droplets and the ambient water vapor/RH. For the NH<sub>4</sub>NO<sub>3</sub>-(NH<sub>4</sub>)<sub>2</sub>SO<sub>4</sub> system, we obtained aerosol particle diameter under different state from the Extended Aerosol Inorganics Model II (E\_AIM) (Clegg et al., 1998), which simulates the state of aerosol system at equilibrium with a given atmospheric temperature and RH conditions based on Köhler theory. The GF at 0–1.0 mole ratio of nitrate was calculated with E\_AIM model data in this study.

## 2.3. Calculation on Aerosol Extinction

Atmospheric aerosol deteriorates regional visibility by absorbing and scattering sun light, whose intensity is highly dependent on the size of particles. Therefore, particle growth due to hygroscopic deliquescence certainly would change the aerosol optical properties and further impair the atmospheric visibility. Such a great importance of aerosol hygroscopic growth has been revealed by many in situ observational and numerical works (Castarède & Thomson, 2018; Kuang et al., 2016; Liu et al., 2008, 2009; Pan et al., 2009; Yoon & Kim, 2006). Extinction coefficient ( $b_{ext}$ ) is the parameter adopted to manifest the radiation attenuation by aerosol particles. With the in situ measured particle number concentration and particle diameter derived from the E\_AIM model, Mie theory was then used to calculate the  $b_{ext}$ . In the Mie theory calculation, the wavelength we used is 589 nm, and at this wavelength the complex refractive indexes of NH<sub>4</sub>NO<sub>3</sub> and (NH<sub>4</sub>)<sub>2</sub>SO<sub>4</sub> are 1.413 + 0i and 1.521 + 0i, respectively (David, 2005). With the calculated result of extinction coefficient, the ratio  $b_{ext(WET)}/b_{ext(DRY)}$  is used to illustrate the increasing of extinction coefficient after hygroscopic deliquescence in this work.

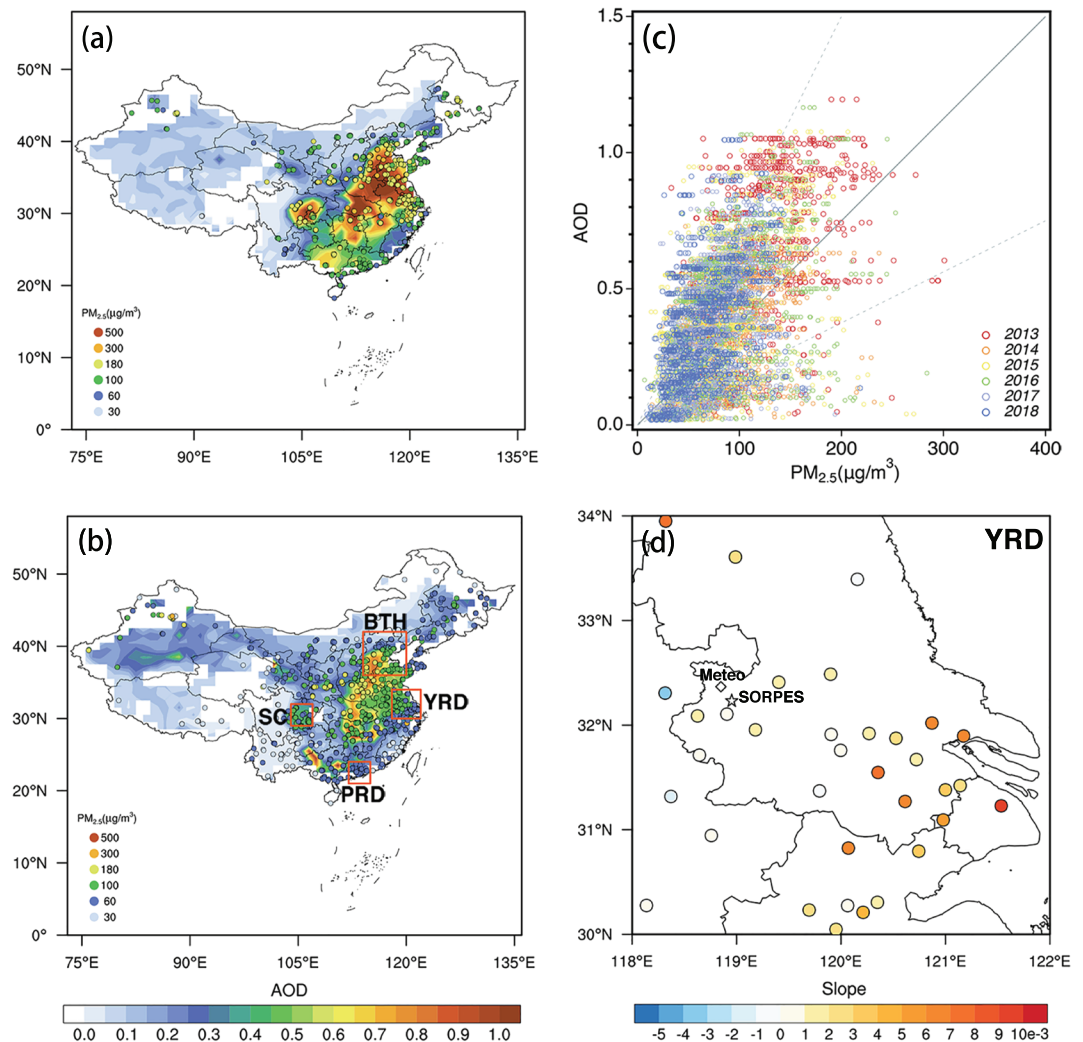


**Figure 1.** Satellite-detected aerosol optical depth (AOD, MOD08) and observed  $PM_{2.5}$  mass concentration (circles) over China in the winter of 2013 (a) and 2018 (b). Red boxes display four representative city clusters (Beijing-Tianjin-Hebei region, the Yangtze River Delta region, the Pearl River Delta region, and the Sichuan-Chongqing region) of China. (c) Scatter plot of AOD versus  $PM_{2.5}$  concentrations at satellite overpass time in 2013–2018 wintertime. The solid 1:1 line and dashed 1:2 and 2:1 lines are shown for reference. (d) Fit slopes of AOD/ $PM_{2.5}$  in the YRD region during 2013–2018 wintertime. Star and diamond symbols mark SORPES and meteorological station, respectively.

Furthermore, to quantitatively understand the relative contribution from different chemical components to aerosol extinction at the SORPES station, the Interagency Monitoring of Protected Visual Environment (IMPROVE) algorithm is also employed to calculate particle extinction coefficient (Chen et al., 2016; Pitchford et al., 2007; Tao et al., 2015). Detailed description of IMPROVE formula is given in supporting information, Text S2.

### 3. Results and Discussions

#### 3.1. Substantial Decline in $PM_{2.5}$ but Less Improved AOD and Visibility

Due to intensive anthropogenic emission and unfavorable meteorological conditions, eastern China has been suffering from frequent and long-lasting haze pollution for long periods, especially in cold seasons (An et al., 2019; Cheng et al., 2013; Fu & Chen, 2016; Wu, 2011; Yang et al., 2016). Owing to the toughest-ever clean air policy across the country since 2013,  $PM_{2.5}$  concentrations have dropped significantly since then. As shown in Figures 1a–1b,  $PM_{2.5}$  of 81% observational sites in 2013 was larger than the daily averaged concentration stipulated by the Grade II Air Quality National Standard ( $75 \mu\text{g}/\text{m}^3$ ).



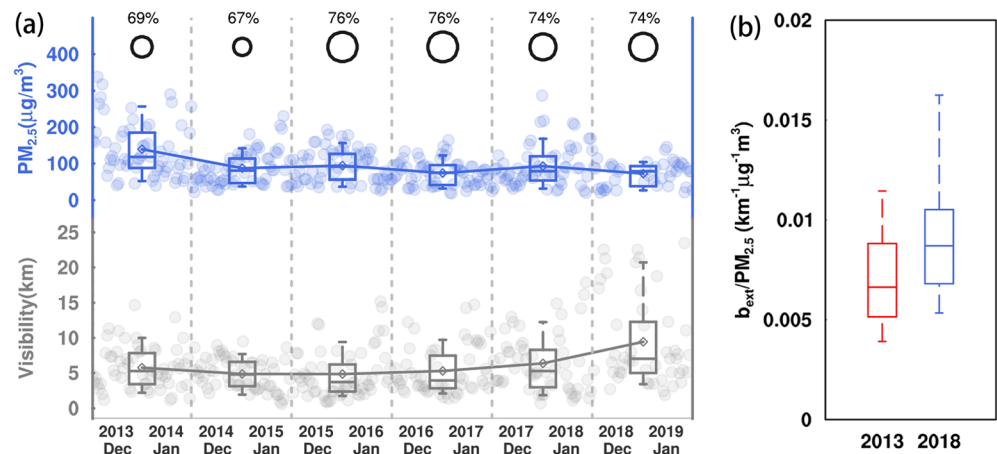


**Figure 2.** (a) Interannual trends in  $PM_{2.5}$  concentration and visibility at the SORPES station in Nanjing during 2013–2018 wintertime (December to January). Circles at the top represent averaged RH in wintertime. (b) Particles mass extinction efficiency in 2013 (red) and 2018 (blue) wintertime. Note that diamond-shaped markers and horizontal lines in the box present the average and median values, the boxes present the 25th and 75th percentiles, and the lower and upper points of dashed lines show the 10th and 90th percentiles, respectively.

Comparatively, only 37% stations recorded an annual mean  $PM_{2.5}$  concentrations over  $75 \mu\text{g}/\text{m}^3$  in 2018. Additionally, the national average of  $PM_{2.5}$  concentration decreased from  $121$  to  $66 \mu\text{g}/\text{m}^3$ , indicating obvious improvements of  $PM_{2.5}$  pollution in recent years. However, the air quality improvement seems not that substantial visually, and haze pollution with low atmospheric visibility still frequently covered eastern China, which is somewhat reflected by a less notable decline in AOD from 2013 to 2018 than expected. As displayed, high values of AOD engulfed a large geographic area over eastern China and Sichuan Basin in 2013, which implies a poor atmospheric visibility (Zhang et al., 2016, 2017). Despite a sharp drop in  $PM_{2.5}$  from 2013 to 2018, the average AOD in China just slightly decreased from 0.24 to 0.21, with some areas barely improved and retained a quite high AOD level in 2018.

Generally, AOD is highly correlated with  $PM_{2.5}$  concentration (Engel-Cox et al., 2004; Wang & Christopher, 2003). Figure 1c shows the relationship between wintertime AOD versus observed  $PM_{2.5}$  concentrations of all stations during 2013–2018. Given the fact that AOD may be influenced by boundary layer height via vertical mixing of aerosol, we further verified that wintertime boundary layer height was comparable during 2013–2018 (supporting information, Figure S1). Here, instead of daily mean concentration, we used  $PM_{2.5}$  concentrations at satellite overpass time to match AOD observation. Similarly, though a sharp decline in  $PM_{2.5}$  was observed between years, AOD showed an inapparent decrease. Notably, compared with 2013, a larger slope between  $PM_{2.5}$  and AOD in 2018 indicates a significant increase in AOD per unit  $PM_{2.5}$  as well as stronger extinction efficiency ( $p < 0.01$  by statistical significance testing). Moreover, the interannual trends of AOD/ $PM_{2.5}$  are well exhibited through the calculated fit slopes from 2013 to 2018 (Figure 1d). In fact, nearly 73.2% stations (939 in 1283 available samples) over China distributed positive slope of AOD/ $PM_{2.5}$ , among which the YRD region featured the most obvious growth trend. That is to say, although  $PM_{2.5}$  mass concentrations have been effectively reduced, the increase of AOD per unit  $PM_{2.5}$  could be indicative of stronger aerosol extinction and thus less improved atmospheric visibility.

The long-term in situ measurements on  $PM_{2.5}$  and atmospheric visibility data were then collected to better understand the interannual variation and their relationship. For the sake of data continuity and better presenting the interannual variation of aerosol and visibility, winter data for one specific year mean the observations in the December and next January. For instance, the December 2018 and January 2019 are considered as the winter of 2018. As shown in Figure 2a, despite the continuous improvement of air quality and atmospheric visibility in Nanjing (one of the typical cities in YRD), the haze was still frequent (frequency of low visibility decreased from 90.2% in 2013 to 67.3% in 2018), and the average visibility remained below 10 km during this period.

Particles mass extinction efficiency (MEE, defined as extinction coefficient ( $b_{ext}$ )/ $PM_{2.5}$ ) is a key parameter representing the extinction intensity of per unit mass  $PM_{2.5}$ . The extinction of particulate matter is related

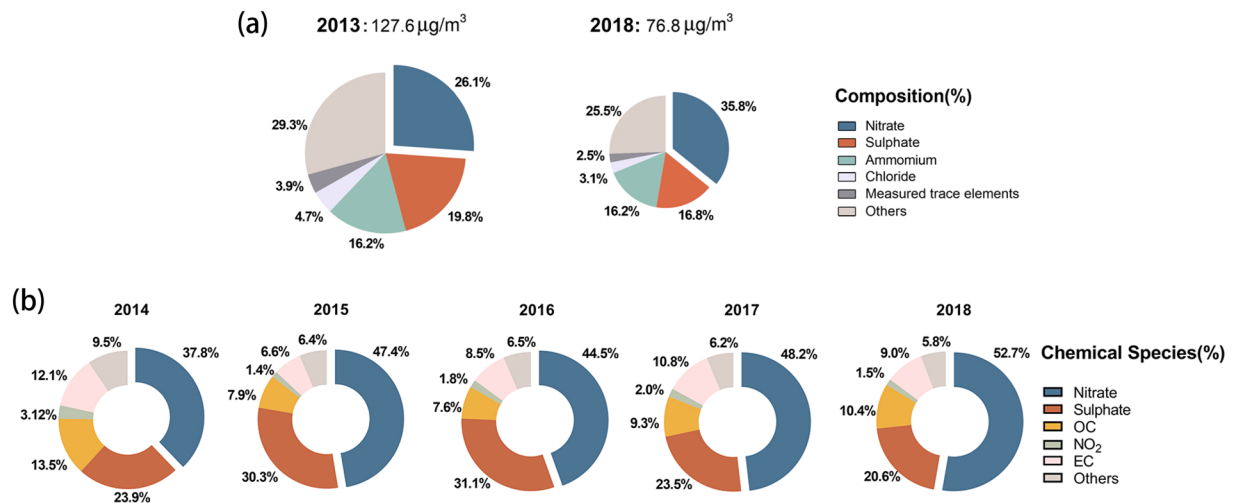


**Figure 3.** (a) Averaged mass concentration of  $\text{PM}_{2.5}$  and the chemical composition (%) measured at the SORPES in Nanjing during 2013 and 2018 wintertime. (b) The individual contributions (%) of different chemical species to extinction coefficient during 2014–2018 wintertime in Nanjing, calculated by IMPROVE formula.

to aerosol hygroscopic deliquescence behavior, which is mainly affected by RH and aerosol compositions (Ding & Liu, 2013; Zhao, Yu, et al., 2019). Due to the increasing capacity of aerosol moisture absorption, MEE is positively correlated with RH (Hyslop, 2009; Liu et al., 2011). As displayed in Figure 2a, the ambient RH showed an increasing trend in recent years, which could partly explain the evident increase of MEE and a stronger aerosol extinction in 2018 compared to 2013 (Figure 2b). Such a nonlinear relationship of  $\text{PM}_{2.5}$  mitigation and visibility degradation then inspires us to further investigate the underlying causes, including the evolution of aerosol composition and humidity condition in past years.

### 3.2. Increasing Proportion of Nitrate in Aerosol Composition

With the emission reduction efforts to mitigate haze pollution in past years,  $\text{PM}_{2.5}$  chemical composition in eastern China has been found to experience an obvious transition, especially secondary inorganic aerosol (SNA) during wintertime (Ding et al., 2019; Li, Cheng, et al., 2019; Wang, Wang, et al., 2019; Zhang, Vu, et al., 2019). Nevertheless, the impact of such a transition on haze pollution and atmospheric visibility has not been fully investigated yet. The long-term observations on aerosol chemical compositions have been conducted in Nanjing since 2013, which are utilized to investigate the evolution of aerosol chemical composition. As shown in Figure 3a, from 2013 to 2018, wintertime concentration of  $\text{PM}_{2.5}$  dropped from 127.6 to

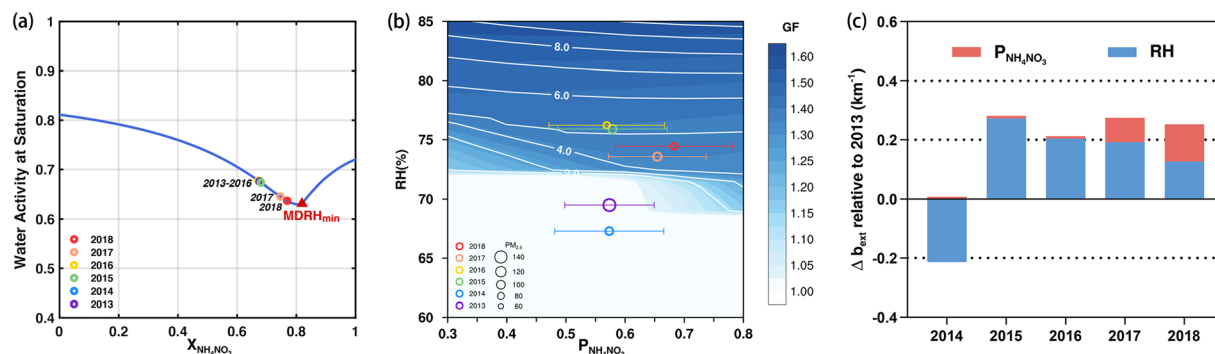


**Figure 4.** (a) Theoretical water activity with different  $X_{\text{NH}_4\text{NO}_3}$  (the relative mole fraction of  $\text{NH}_4\text{NO}_3$  in aerosol) at saturation of an aqueous solution of  $\text{NH}_4\text{NO}_3$  and  $(\text{NH}_4)_2\text{SO}_4$  at 283 K. The wintertime  $X_{\text{NH}_4\text{NO}_3}$  from 2013 to 2018 is marked on the curve. (b) Evolution of wintertime particle growth factor (GF, contour shadow) and extinction coefficient growth factor (ECGF, contour line) in Nanjing from 2013 to 2018. The mass ratios of  $\text{NH}_4\text{NO}_3$ , RH, and  $\text{PM}_{2.5}$  concentrations (circle size) are based on observational data during 2013–2018 wintertime at the SORPES station in Nanjing. Notice that the x-axis ( $P_{\text{NH}_4\text{NO}_3}$ ) represents the mass proportion of  $\text{NH}_4\text{NO}_3$  for a better comparison with field observations and the y-axis represents the ambient RH. (c) The relative contributions from nitrate proportion and RH to changes in aerosol extinction during 2014–2018.

76.8  $\mu\text{g}/\text{m}^3$ , approximately decreased by 40%. Furthermore, due to the unbalanced emission reduction of  $\text{NO}_x$  and  $\text{SO}_2$  (supporting information, Figure S2), the mass proportion of nitrate in  $\text{PM}_{2.5}$  evidently increased from 26.1% to 35.8%, making it the most important contributor to  $\text{PM}_{2.5}$  mass concentration. The similar transition of  $\text{PM}_{2.5}$  compositions has also been reported in other regions. For example, the mass fraction of nitrate in  $\text{PM}_{2.5}$  mass concentration increased from 19% to 30% in Beijing during 2013–2018 (Xu et al., 2019) and from 12.9% to 23.4% in Guangzhou during 2013–2015 (Wang, Li, et al., 2019). The increasing nitrate in these regions has been attributed to distinct emission control on  $\text{NO}_x$  and  $\text{SO}_2$  confirmed by both model and observational studies (Fu et al., 2020; Xu et al., 2019). Specifically, the oxidation products of  $\text{NO}_x$  and  $\text{SO}_2$ , i.e., nitric acid and sulfuric acid, compete in the combination with ambient ammonia (Wang et al., 2012). Owing to the much more efficient emission control of  $\text{SO}_2$ , sulfate decreased sharply and resulted in a surplus of ammonia in the atmosphere, which further neutralized nitric acid to form  $\text{NH}_4\text{NO}_3$ , thereby elevating the proportion of nitrate in particles (Lachatre et al., 2019; Liu et al., 2018).

It is noteworthy that various chemical species contribute differently to visibility degradation (Huang et al., 2014; Kim et al., 2006; Ouimette & Flagan, 1982; Yu et al., 2018). Hand and Malm (2006) analyzed the correlation between aerosol and visibility based on the IMPROVE monitoring network, indicating that sulfate, nitrate, organic matter, light-absorbing carbon, sand dust, and  $\text{NO}_2$  gas are the main chemical components for visibility impairment. Then, IMPROVE algorithm, which was proposed by Pitchford et al. (2007), was used to quantify the contributions from various chemical components to total aerosol extinction. Figure 3b illustrated that nitrate was the most important contributor, accounting for 40%–50% of aerosol extinction. The dominance of SNA in aerosol extinction (i.e., a remarkably high contribution ranging 50% to 80%) has been revealed in many regions, which was proven to play a major role in visibility degradation and regional haze pollution (Han et al., 2017; Tan et al., 2009; Wang et al., 2012). Clearly, nitrate portion in aerosol mass concentration was characterized by an increasing trend from 2013 to 2018, indicating that non-obvious visibility improvement might be attributed to a rising nitrate.

### 3.3. Higher Aerosol Hygroscopicity and Extinction Efficiency

In addition to aerosol chemical composition, the hygroscopic growth also plays a crucial role in aerosol extinction, which is mainly determined by hygroscopic inorganic salts. In fact, the hygroscopic inorganic salts in aerosol are mainly ammonium sulfate and ammonium nitrate, fairly common constituents of atmospheric aerosols in China due to the intensive emissions of precursors (Wu et al., 2019; Zawadowicz et al., 2015). Previous studies already suggested the vital role of aerosol composition transition on hygroscopicity and extinction (Kuang et al., 2016; Wang et al., 2017; Xu et al., 2020). To shed more light on it, we further conducted the theoretical calculation for the MDRH of hydrophilic aerosol consisting of  $\text{NH}_4\text{NO}_3$  and  $(\text{NH}_4)_2\text{SO}_4$ , as described in section 2.2. Figure 4a shows the water activity of saturated aqueous solution consists of  $\text{NH}_4\text{NO}_3$  and  $(\text{NH}_4)_2\text{SO}_4$ , that is the crucial RH for aerosol to transform from solid to liquid, under different  $X_{\text{NH}_4\text{NO}_3}$  (the relative mole fraction of  $\text{NH}_4\text{NO}_3$ ) of 2013–2018 wintertime in Nanjing. As shown, with the increasing proportion of ammonium nitrate, the critical deliquescence RH value of aerosol system showed a declining trend until the ammonium nitrate reaching a certain high proportion at the red triangle (the minimum MDRH,  $X_{\text{NH}_4\text{NO}_3} = 0.82$ ). The MDRH and ambient RH jointly determine whether the aerosols can completely deliquesce. Notably, decrease in the critical RH value would raise the number of aerosols in deliquescent state at the same level of ambient RH, resulting in a larger particle size and then enhanced aerosol extinction efficiency. Accordingly, the evidently increased nitrate proportion in Nanjing during 2013–2018 would directly lead to the decrease in deliquescence RH, that is, a lower ambient RH requirement for hygroscopic growth.

Aerosol hygroscopicity directly determines its extinction efficiency via changing particle diameter. Based on the E\_AIM model, we calculated the particle size GF and the extinction coefficient growth factor (ECGF) for quantifying aerosol hygroscopic and optical properties, respectively. As presented in Figure 4b, with an increasing mass proportion of ammonium nitrate ( $P_{\text{NH}_4\text{NO}_3}$ ) from 0.3 to 0.8, GF and ECGF showed an increasing trend at the same ambient RH, especially within the RH range of 70%–75%, indicating a stronger aerosol extinction due to a larger nitrate fraction. Meanwhile, the increase in ambient RH condition also enhanced aerosol hygroscopicity and extinction. Statistically, the values of GF and ECGF were estimated to be about 1.4 and 4.7 in 2018, obviously larger than those in 2013, demonstrating that despite a significant decline in  $\text{PM}_{2.5}$  concentration, aerosol hygroscopicity and extinction in 2018 are stronger than those before

due to higher nitrate fraction and RH condition. The thermodynamic calculation was then conducted for the time period from 2013 to 2018 in order to estimate the respective contributions from these two factors. It is worth noting that the hygroscopic behavior of ambient aerosol is much more complex than theoretical calculation due to many other influencing factors like size distribution and hygroscopicity of organic matters, and Figures 4c and S3 just give a statistical estimation. It is indicated that RH variations dominated the aerosol extinction change in the first 3 years. With a gradually rising fraction of nitrate, transition in aerosol chemical composition and RH increase contributed comparably to the enhanced aerosol extinction after 2017. Overall, in situ measurements, theoretical analysis, and model simulations are indicative of a stronger aerosol hygroscopicity caused by the increasing nitrate fraction and ambient RH, which would enhance aerosol extinction and further hinder the visibility improvement. In consequence, the efforts of substantial reduction in  $PM_{2.5}$  could be partly offset.

#### 4. Summary

In this work, by combining long-term observations of meteorological parameters,  $PM_{2.5}$ , and its chemical compositions, we found a continuous decrease in  $PM_{2.5}$  mass concentration but an inapparent improvement of atmospheric visibility in eastern China from 2013 to 2018. In addition, nitrate has become the dominant species in  $PM_{2.5}$ , and its mass fraction increased from 26.1% to 35.8% from 2013 to 2018. We further conducted aerosol thermodynamic modeling and theoretical calculation to understand the relationship between  $PM_{2.5}$  variation and atmospheric visibility improvement. It is found that the increasing proportion of nitrate in aerosol and higher RH in past years would enhance aerosol hygroscopicity as well as aerosol extinction efficiency. Such a transition in aerosol chemical compositions together with increasing ambient humidity resulted in the less improved visibility despite great emission control effort in eastern China. Further, change in aerosol composition and RH would exert vital influence on aerosol extinction through varying hygroscopic growth, which is of critical importance for haze predictions and simulations. Multipollutant control, especially more reduction on  $NO_x$  emission, may serve as an effective way to further improve visibility.

#### Data Availability Statement

Measurements on air quality data across China are collected through the online access to ambient air monitoring data center and are available online (<https://doi.org/10.6084/m9.figshare.12765689>). Satellite data on aerosol optical depth are available online ([https://doi.org/10.5067/MODIS/MOD08\\_M3.006](https://doi.org/10.5067/MODIS/MOD08_M3.006)).

#### Acknowledgments

This work was supported by the National Natural Science Foundation of China (41922038, 41875150, 41725020, and 91744311).

#### References

- An, Z., Huang, R.-J., Zhang, R., Tie, X., Li, G., Cao, J., et al. (2019). Severe haze in northern China: A synergy of anthropogenic emissions and atmospheric processes. *Proceedings of the National Academy of Sciences of the United States of America*, *116*(18), 8657–8666. <http://doi.org/10.1073/pnas.1900125116>
- Brook, R. D., Rajagopalan, S., Pope, C. A., Brook, J. R., Bhatnagar, A., Diez-Roux, A. V., et al. (2010). Particulate matter air pollution and cardiovascular disease: An update to the scientific statement from the American Heart Association. *Circulation*, *121*(21), 2331–2378. <https://doi.org/10.1161/CIR.0b013e3181d8e1>
- Castarède, D., & Thomson, E. S. (2018). A thermodynamic description for the hygroscopic growth of atmospheric aerosol particles. *Atmospheric Chemistry and Physics*, *18*(20), 14,939–14,948. <http://doi.org/10.5194/acp-18-14939-2018>
- Chang, D., Song, Y., & Liu, B. (2009). Visibility trends in six megacities in China 1973–2007. *Atmospheric Research*, *94*(2), 161–167. <http://doi.org/10.1016/j.atmosres.2009.05.006>
- Chen, X., Lai, S., Gao, Y., Zhang, Y., Zhao, Y., Chen, D., et al. (2016). Reconstructed light extinction coefficients of fine particulate matter in rural Guangzhou, Southern China. *Aerosol and Air Quality Research*, *16*(8), 1981–1990. <http://doi.org/10.4209/aaqr.2016.02.0064>
- Cheng, Z., Wang, S., Jiang, J., Fu, Q., Chen, C., Xu, B., et al. (2013). Long-term trend of haze pollution and impact of particulate matter in the Yangtze River Delta, China. *Environmental Pollution Barking, Essex: 1987*, *182*, 101–110. <http://doi.org/10.1016/j.envpol.2013.06.043>
- China State Council (2013). *Action plan on prevention and control of air pollution*. Beijing, China: China State Council. (In Chinese)
- Clegg, S., Brimblecombe, P., & Wexler, A. (1998). Thermodynamic model of the system  $H^+ - NH_4^+ - Na^+ - SO_4^{2-} - NO_3^- - Cl^- - H_2O$  at 298.15 K. *Journal of Physical Chemistry A*, *102*(12), 2155–2171. <http://doi.org/10.1021/jp973043j>
- David, R. L. (2005). Analytical chemistry. *CRC handbook of chemistry and physics* (Internet Version 2005, pp. 8–60). Boca Raton, FL: CRC Press.
- Ding, A. J., Fu, C. B., Yang, X. Q., Sun, J. N., Zheng, L. F., Xie, Y. N., et al. (2013). Ozone and fine particle in the western Yangtze River Delta: An overview of 1 yr data at the SORPES station. *Atmospheric Chemistry and Physics*, *13*(11), 5813–5830. <http://doi.org/10.5194/acp-13-5813-2013>
- Ding, A. J., Huang, X., Nie, W., Chi, X., Xu, Z., Zheng, L., et al. (2019). Significant reduction of PM 2.5 in eastern China due to regional-scale emission control: Evidence from SORPES in 2011–2018. *Atmospheric Chemistry and Physics*, *19*(18), 11,791–11,801. <http://doi.org/10.5194/acp-19-11791-2019>



- Ding, A. J., Huang, X., Nie, W., Sun, J., Kerminen, V.-M., Petäjä, T., et al. (2016). Black carbon enhances haze pollution in megacities in China. *Geophysical Research Letters*, *43*, 2873–2879. <http://doi.org/10.1002/2016GL067745>
- Ding, Y., & Liu, Y. (2013). Analysis of long-term variations of fog and haze in China in recent 50 years and their relations with atmospheric humidity. *Science China Earth Sciences*, *57*(1), 36–46. <http://doi.org/10.1007/s11430-013-4792-1>
- Engel-Cox, J., Holloman, C., Coutant, B., & Hoff, R. (2004). Qualitative and quantitative evaluation of MODIS satellite sensor data for regional and urban scale air quality. *Atmospheric Environment*, *38*(16), 2495–2509. <http://doi.org/10.1016/j.atmosenv.2004.01.039>
- Fu, H., & Chen, J.-M. (2016). Formation, features and controlling strategies of severe haze-fog pollutions in China. *Science of the Total Environment*, *578*, 121–138. <http://doi.org/10.1016/j.scitotenv.2016.10.201>
- Fu, X., Wang, T., Gao, J., Wang, P., Liu, Y., Wang, S., et al. (2020). Persistent heavy winter nitrate pollution driven by increased photochemical oxidants in northern China. *Environmental Science & Technology*, *54*(7), 3881–3889. <http://doi.org/10.1021/acs.est.9b07248>
- Han, T., Xu, W., Li, J., Freedman, A., Zhao, J., Wang, Q., et al. (2017). Aerosol optical properties measurements by a CAPS single scattering albedo monitor: Comparisons between summer and winter in Beijing, China: Aerosol optical properties in Beijing. *Journal of Geophysical Research: Atmospheres*, *122*, 2513–2526. <http://doi.org/10.1002/2016JD025762>
- Hand, J. L., & Malm, W. C. (2006). Review of the IMPROVE equation for estimating ambient light extinction coefficients-Final Report. Fort Collins, CO: Interagency Monitoring of Protected Visual Environments. Retrieved from [http://vista.cira.colostate.edu/IMPROVE/Publications/GrayLit/016\\_IMPROVEeqReview/IMPROVEeqReview.htm](http://vista.cira.colostate.edu/IMPROVE/Publications/GrayLit/016_IMPROVEeqReview/IMPROVEeqReview.htm)
- Huang, R.-J., Zhang, Y., Bozzetti, C., Ho, K.-F., Cao, J.-J., Han, Y., et al. (2014). High secondary aerosol contribution to particulate pollution during haze events in China. *Nature*, *514*(7521), 218–222. <http://doi.org/10.1038/nature13774>
- Huang, X., Ding, A., Gao, J., Zheng, B., Zhou, D., Qi, X., et al. (2020). Enhanced secondary pollution offset reduction of primary emissions during COVID-19 lockdown in China. *National Science Review*. <http://doi.org/10.1093/nsr/nwaa137>
- Huang, X., Ding, A., Wang, Z., Ding, K., Gao, J., Chai, F., & Fu, C. (2020). Amplified transboundary transport of haze by aerosol–boundary layer interaction in China. *Nature Geoscience*, *13*(6), 428–434. <http://doi.org/10.1038/s41561-020-0583-4>
- Huang, X., Song, Y., Li, M., Li, J., Huo, Q., Cai, X., et al. (2012). A high-resolution ammonia emission inventory in China. *Global Biogeochemical Cycles*, *26*, 1030. <http://doi.org/10.1029/2011GB004161>
- Hyslop, N. P. (2009). Impaired visibility: The air pollution people see. *Atmospheric Environment*, *43*(1), 182–195. <http://doi.org/10.1016/j.atmosenv.2008.09.067>
- Kim, K.-H., Kabir, E., & Kabir, S. (2015). A review on the human health impact of airborne particulate matter. *Environment International*, *74*, 136–143. <http://doi.org/10.1016/j.envint.2014.10.005>
- Kim, Y. J., Kim, K. W., Kim, S. D., Lee, B. K., & Han, J. S. (2006). Fine particulate matter characteristics and its impact on visibility impairment at two urban sites in Korea: Seoul and Incheon. *Atmospheric Environment*, *40*, 593–S605. <http://doi.org/10.1016/j.atmosenv.2005.11.076>
- Kuang, Y., Zhao, C. S., Ma, N., Liu, H. J., Bian, Y. X., Tao, J. C., & Hu, M. (2016). Deliquescent phenomena of ambient aerosols on the North China Plain. *Geophysical Research Letters*, *43*, 8744–8750. <http://doi.org/10.1002/2016gl070273>
- Lachatre, M., Fortems-Cheiney, A., Foret, G., Siour, G., Dufour, G., Clarisse, L., et al. (2019). The unintended consequence of SO<sub>2</sub> and NO<sub>2</sub> regulations over China: Increase of ammonia levels and impact on PM<sub>2.5</sub> concentrations. *Atmospheric Chemistry and Physics*, *19*(10), 6701–6716. <http://doi.org/10.5194/acp-19-6701-2019>
- Li, H., Cheng, J., Zhang, Q., Zheng, B., Zhang, Y., Zheng, G., & He, K. (2019). Rapid transition in winter aerosol composition in Beijing from 2014 to 2017: Response to clean air actions. *Atmospheric Chemistry and Physics*, *19*(17), 11,485–11,499. <http://doi.org/10.5194/acp-19-11485-2019>
- Li, J., Li, C., Zhao, C., & Su, T. (2016). Changes in surface aerosol extinction trends over China during 1980–2013 inferred from quality-controlled visibility data. *Geophysical Research Letters*, *43*, 8713–8719. <http://doi.org/10.1002/2016GL070201>
- Li, J., Liao, H., Hu, J., & Li, N. (2019). Severe particulate pollution days in China during 2013–2018 and the associated typical weather patterns in Beijing-Tianjin-Hebei and the Yangtze River Delta regions. *Environmental Pollution*, *248*(2), 74–81. <https://doi.org/10.1016/j.envpol.2019.01.124>
- Liu, M., Huang, X., Song, Y., Xu, T., Wang, S., Wu, Z., et al. (2018). Rapid SO<sub>2</sub> emission reductions significantly increase tropospheric ammonia concentrations over the North China Plain. *Atmospheric Chemistry and Physics*, *18*(24), 17,933–17,943. <http://doi.org/10.5194/acp-18-17933-2018>
- Liu, P. F., Zhao, C. S., Goebel, T., Hallbauer, E., Nowak, A., Ran, L., et al. (2011). Hygroscopic properties of aerosol particles at high relative humidity and their diurnal variations in the North China Plain. *Atmospheric Chemistry and Physics*, *11*(7), 3479–3494. <http://doi.org/10.5194/acp-11-3479-2011>
- Liu, X., Cheng, Y., Zhang, Y., Jung, J., Sugimoto, N., Chang, S.-Y., et al. (2008). Influences of relative humidity and particle chemical composition on aerosol scattering properties during the 2006 PRD campaign. *Atmospheric Environment*, *42*(7), 1525–1536. <http://doi.org/10.1016/j.atmosenv.2007.10.077>
- Liu, X., Zhang, Y., Jung, J., Gu, J., Li, Y., Guo, S., et al. (2009). Research on the hygroscopic properties of aerosols by measurement and modeling during CAREBeijing-2006. *Journal of Geophysical Research*, *114*, D00G16. <http://doi.org/10.1029/2008JD010805>
- Liu, Y., Wu, Z., Huang, X., Shen, H., Bai, Y., Qiao, K., et al. (2019). Aerosol phase state and its link to chemical composition and liquid water content in a subtropical coastal megacity. *Environmental Science & Technology*, *53*(9), 5027–5033. <http://doi.org/10.1021/acs.est.9b01196>
- Malm, W. C., & Kreidenweis, S. M. (1997). The effects of models of aerosol hygroscopicity on the apportionment of extinction. *Atmospheric Environment*, *31*(13), 1965–1976. [http://doi.org/10.1016/s1352-2310\(96\)00355-x](http://doi.org/10.1016/s1352-2310(96)00355-x)
- Ouimette, J., & Flagan, R. (1982). The extinction coefficient of multicomponent aerosols. *Atmospheric Environment*, *16*, 2405–2419. [http://doi.org/10.1016/0004-6981\(82\)90131-7](http://doi.org/10.1016/0004-6981(82)90131-7)
- Pan, X. L., Yan, P., Tang, J., Ma, J. Z., Wang, Z. F., Gbaguidi, A., & Sun, Y. L. (2009). Observational study of influence of aerosol hygroscopic growth on scattering coefficient over rural area near Beijing mega-city. *Atmospheric Chemistry and Physics*, *9*(19), 7519–7530. <http://doi.org/10.5194/acp-9-7519-2009>
- Pitchford, M., Malm, W., Schichtel, B., Kumar, N., Lowenthal, D., & Hand, J. (2007). Revised algorithm for estimating light extinction from IMPROVE particle speciation data. *Journal of the Air & Waste Management Association*, *57*(11), 1326–1336. <http://doi.org/10.3155/1047-3289.57.11.1326>
- Qi, X. M., Ding, A. J., Nie, W., Petaja, T., Kerminen, V. M., Herrmann, E., et al. (2015). Aerosol size distribution and new particle formation in the western Yangtze River Delta of China: 2 years of measurements at the SORPES station. *Atmospheric Chemistry and Physics*, *15*(21), 12,445–12,464. <http://doi.org/10.5194/acp-15-12445-2015>
- Seinfeld, J. H., & Pandis, S. N. (2016). Thermodynamics of aerosols. *Atmospheric chemistry and physics: From air pollution to climate change* (3rd ed., pp. 412–414). Hoboken, NJ: John Wiley.

- Shen, Y., Virkkula, A., Ding, A., Wang, J., Chi, X., Nie, W., et al. (2018). Aerosol optical properties at SORPES in Nanjing, East China. *Atmospheric Chemistry and Physics*, 18(8), 5265–5292. <http://doi.org/10.5194/acp-18-5265-2018>
- Tan, J.-H., Duan, J.-C., Chen, D.-H., Wang, X.-H., Guo, S.-J., Bi, X.-H., et al. (2009). Chemical characteristics of haze during summer and winter in Guangzhou. *Atmospheric Research*, 94(2), 238–245. <http://doi.org/10.1016/j.atmosres.2009.05.016>
- Tang, M., Gu, W., Ma, Q., Li, Y. J., Zhong, C., Li, S., et al. (2019). Water adsorption and hygroscopic growth of six anemophilous pollen species: The effect of temperature. *Atmospheric Chemistry and Physics*, 19(4), 2247–2258. <http://doi.org/10.5194/acp-19-2247-2019>
- Tao, J., Zhang, L., Zhang, Z., Huang, R., Wu, Y., Zhang, R., et al. (2015). Control of PM<sub>2.5</sub> in Guangzhou during the 16th Asian Games period: Implication for hazy weather prevention. *Science of the Total Environment*, 508, 57–66. <http://doi.org/10.1016/j.scitotenv.2014.11.074>
- Tombach, I., & McDonald, K. (2004). Visibility and radiative balance effects. In P. McMurry, M. Shepherd, J. Vickery (Eds.), *Particulate matter science for policy makers: A NARSTO assessment* (pp. 325–354). Cambridge, MA: Cambridge University Press.
- Wang, J., & Christopher, S. A. (2003). Intercomparison between satellite-derived aerosol optical thickness and PM<sub>2.5</sub> mass: Implications for air quality studies. *Geophysical Research Letters*, 30(21), 2095. <http://doi.org/10.1029/2003GL018174>
- Wang, J., Nie, W., Cheng, Y., Shen, Y., Chi, X., Wang, J., et al. (2018). Light absorption of brown carbon in eastern China based on 3-year multi-wavelength aerosol optical property observations and an improved absorption Angstrom exponent segregation method. *Atmospheric Chemistry and Physics*, 18(12), 9061–9074. <http://doi.org/10.5194/acp-18-9061-2018>
- Wang, N., Lyu, X., Deng, X., Huang, X., Jiang, F., & Ding, A. (2019). Aggravating O<sub>3</sub> pollution due to NO<sub>x</sub> emission control in eastern China. *Science of the Total Environment*, 677, 732–744. <http://doi.org/10.1016/j.scitotenv.2019.04.388>
- Wang, X., Wang, W., Yang, L., Gao, X., Nie, W., Yu, Y., et al. (2012). The secondary formation of inorganic aerosols in the droplet mode through heterogeneous aqueous reactions under haze conditions. *Atmospheric Environment*, 63, 68–76. <http://doi.org/10.1016/j.atmosenv.2012.09.029>
- Wang, Y., Li, W., Gao, W., Liu, Z., Tian, S., Shen, R., et al. (2019). Trends in particulate matter and its chemical compositions in China from 2013–2017. *Science China Earth Sciences*, 62(12), 1857–1871. <https://doi.org/10.1007/s11430-018-9373-1>
- Wang, Y., Wang, Q., Ye, J., Yan, M., Qin, Q., Prevot, A. S. H., & Cao, J. (2019). A review of aerosol chemical composition and sources in representative regions of China during wintertime. *Atmosphere*, 10(5), 277. <http://doi.org/10.3390/atmos10050277>
- Wang, Y., Zhang, F., Li, Z., Tan, H., Xu, H., Ren, J., et al. (2017). Enhanced hydrophobicity and volatility of submicron aerosols under severe emission control conditions in Beijing. *Atmospheric Chemistry and Physics*, 17(8), 5239–5251. <http://doi.org/10.5194/acp-17-5239-2017>
- Wexler, A., & Seinfeld, J. (1991). Second-generation inorganic aerosol model. *Atmospheric Environment. Part A. General Topics*, 25A, 2731–2748. [http://doi.org/10.1016/0960-1686\(91\)90203-J](http://doi.org/10.1016/0960-1686(91)90203-J)
- World Health Organization (2006). WHO Air quality guidelines for particulate matter, ozone, nitrogen dioxide and sulfur dioxide: Global update 2005: Summary of risk assessment.
- Wu, D. (2011). Formation and evolution of haze weather. *Environmental Science & Technology*, 34(3), 157–161.
- Wu, L., Li, X., & Ro, C.-U. (2019). Hygroscopic behavior of ammonium sulfate, ammonium nitrate, and their mixture particles. *Asian Journal of Atmospheric Environment*, 13(3), 196–211. <http://doi.org/10.5572/ajae.2019.13.3.196>
- Xie, Y., Ding, A., Nie, W., Mao, H., Qi, X., Huang, X., et al. (2015). Enhanced sulfate formation by nitrogen dioxide: Implications from in situ observations at the SORPES station. *Journal of Geophysical Research: Atmospheres*, 120, 12,679–12,694. <http://doi.org/10.1002/2015JD023607>
- Xu, Q., Wang, S., Jiang, J., Bhattarai, N., Li, X., Chang, X., et al. (2019). Nitrate dominates the chemical composition of PM<sub>2.5</sub> during haze event in Beijing, China. *Science of the Total Environment*, 689, 1293–1303. <http://doi.org/10.1016/j.scitotenv.2019.06.294>
- Xu, W., Kuang, Y., Bian, Y., Liu, L., Li, F., Wang, Y., et al. (2020). Current challenges in visibility improvement in southern China. *Environmental Science & Technology Letters*, 7(6), 395–401. <http://doi.org/10.1021/acs.estlett.0c00274>
- Yang, Y., Liao, H., & Lou, S. (2016). Increase in winter haze over eastern China in recent decades: Roles of variations in meteorological parameters and anthropogenic emissions. *Journal of Geophysical Research: Atmospheres*, 121, 13,050–13,065. <http://doi.org/10.1002/2016JD025136>
- Yoon, S.-C., & Kim, J. (2006). Influences of relative humidity on aerosol optical properties and aerosol radiative forcing during ACE-Asia. *Atmospheric Environment*, 40(23), 4328–4338. <http://doi.org/10.1016/j.atmosenv.2006.03.036>
- Yu, Y., Zhao, C., Kuang, Y., Tao, J., Zhao, G., Shen, C., & Xu, W. (2018). A parameterization for the light scattering enhancement factor with aerosol chemical compositions. *Atmospheric Environment*, 191, 370–377. <http://doi.org/10.1016/j.atmosenv.2018.08.016>
- Zawadowicz, M., Proud, S., Seppäläinen, S., & Cziczo, D. (2015). Hygroscopic and phase separation properties of ammonium sulfate/organics/water ternary solutions. *Atmospheric Chemistry and Physics*, 15(15), 8975–8986. <http://doi.org/10.5194/acp-15-8975-2015>
- Zhang, Q., He, K., & Huo, H. (2012). Cleaning China's air. *Nature*, 484(7393), 161–162. <http://doi.org/10.1038/484161a>
- Zhang, Q., Quan, J., Tie, X., Li, X., Liu, Q., Gao, Y., & Zhao, D. (2015). Effects of meteorology and secondary particle formation on visibility during heavy haze events in Beijing, China. *Science of the Total Environment*, 502, 578–584. <http://doi.org/10.1016/j.scitotenv.2014.09.079>
- Zhang, Q., Zheng, Y., Tong, D., Shao, M., Wang, S., Zhang, Y., et al. (2019). Drivers of improved PM<sub>2.5</sub> air quality in China from 2013 to 2017. *Proceedings of the National Academy of Sciences*, 116(49), 24,463–24,469. <http://doi.org/10.1073/pnas.1907956116>
- Zhang, Y., Vu, T. V., Sun, J., He, J., Shen, X., Lin, W., et al. (2019). Significant changes in chemistry of fine particles in wintertime Beijing from 2007 to 2017: Impact of clean air actions. *Environmental Science & Technology*, 54(3), 1344–1352. <http://doi.org/10.1021/acs.est.9b04678>
- Zhang, Z. Y., Wong, M. S., & Lee, K. H. (2016). Evaluation of the representativeness of ground-based visibility for analysing the spatial and temporal variability of aerosol optical thickness in China. *Atmospheric Environment*, 147, 31–45. <http://doi.org/10.1016/j.atmosenv.2016.09.060>
- Zhang, Z. Y., Wu, W., Wei, J., Song, Y., Yan, X., Zhu, L., & Wang, Q. (2017). Aerosol optical depth retrieval from visibility in China during 1973–2014. *Atmospheric Environment*, 171, 38–48. <http://doi.org/10.1016/j.atmosenv.2017.09.004>
- Zhao, C., Yu, Y., Kuang, Y., Tao, J., & Zhao, G. (2019). Recent progress of aerosol light-scattering enhancement factor studies in China. *Advances in Atmospheric Sciences*, 36(9), 1015–1026. <http://doi.org/10.1007/s00376-019-8248-1>
- Zhao, L., Wang, L., Tan, J., Duan, J., Ma, X., Zhang, C., et al. (2019). Changes of chemical composition and source apportionment of PM<sub>2.5</sub> during 2013–2017 in urban Handan, China. *Atmospheric Environment*, 206, 119–131. <http://doi.org/10.1016/j.atmosenv.2019.02.034>
- Zheng, B., Tong, D., Li, M., Liu, F., Hong, C., Geng, G., et al. (2018). Trends in China's anthropogenic emissions since 2010 as the consequence of clean air actions. *Atmospheric Chemistry and Physics*, 18(19), 14,095–14,111. <http://doi.org/10.5194/acp-18-14095-2018>

- Zheng, G., Duan, F., Ma, Y., Zhang, Q., Huang, T., Kimoto, T., et al. (2016). Episode-based evolution pattern analysis of haze pollution: Method development and results from Beijing, China. *Environmental Science & Technology*, *50*(9), 4632–4641. <http://doi.org/10.1021/acs.est.5b05593>
- Zou, J., Liu, Z., Hu, B., Huang, X., Wen, T., Ji, D., et al. (2018). Aerosol chemical compositions in the North China Plain and the impact on the visibility in Beijing and Tianjin. *Atmospheric Research*, *201*, 235–246. <https://doi.org/10.1016/j.atmosres.2017.09.014>